AIP | Applied Physics Letters

Improved power conversion efficiency of InP solar cells using organic window layers

Ning Li, Kyusang Lee, Christopher K. Renshaw, Xin Xiao, and Stephen R. Forrest

Citation: Appl. Phys. Lett. **98**, 053504 (2011); doi: 10.1063/1.3549692
View online: http://dx.doi.org/10.1063/1.3549692
View Table of Contents: http://apl.aip.org/resource/1/APPLAB/v98/i5
Published by the AIP Publishing LLC.

Improved power conversion efficiency of InP solar cells using organic window layers

Ning Li, Kyusang Lee, Christopher K. Renshaw, Xin Xiao, and Stephen R. Forrest[a)]
Departments of Electrical Engineering and Computer Science, Materials Science and Engineering, and Physics, University of Michigan, Ann Arbor, Michigan 48109, USA

(Received 28 November 2010; accepted 8 January 2011; published online 2 February 2011)

We employ the organic semiconductor 3,4,9,10-perylene-tetracarboxylic-dianhydride (PTCDA) as a nanometer thick window layer for p-InP/indium tin oxide (ITO) Schottky barrier diode solar cells. The power conversion efficiency is enhanced compared to ITO/InP cells lacking the PTCDA window layer, primarily due to neutralizing InP surface state charges via hole injection from the PTCDA. This leads to an increased ITO/p-InP Schottky barrier height, and hence to an increased open circuit voltage. The power conversion efficiency of the cells increases from $13.2 \pm 0.5\%$ for the ITO/InP cell to $15.4 \pm 0.4\%$ for the ITO/4 nm PTCDA/p-InP cell under 1 sun, AM1.5G simulated solar illumination. The PTCDA window layer is also shown to contribute to the photocurrent by light absorption followed by exciton dissociation at the organic/inorganic semiconductor interface. © *2011 American Institute of Physics*. [doi:10.1063/1.3549692]

The performance of inorganic solar cells can be enhanced using large bandgap semiconductor windows known as heterocontact layers.[1–7] These layers can improve the solar cell photocurrent and open circuit voltage in both Schottky barrier[1] and p-n junction[5] devices, primarily by reducing the effects of surface states at the contact/semiconductor interface. The window layer is often comprised of lattice matched III-V compounds grown on the GaAs and InP surfaces,[2] metal-oxides, or amorphous semiconductors.[4–7]

Here we show that using an organic semiconductor window layer in an otherwise conventional metal/InP Schottky diode can also improve solar cell performance, but with reduced fabrication complexity and without the requirement for epitaxial growth encountered in layered inorganic p-n junctions.[1] This work is based on the previous observation that deposition of the archetype organic semiconductor 3,4,9,10-perylene-tetracarboxylic-dianhydride (PTCDA) between a metal electrode and InP results in a significant increase in the interface barrier height (ϕ_B) as compared with an analogous Schottky-type metal/InP junction.[8,9] We also show that excitons generated in the PTCDA dissociate at the organic-inorganic (OI) semiconductor heterojunction, thereby contributing to the photocurrent of the solar cell.[10] By adding a thin layer of PTCDA between an indium tin oxide (ITO) cathode and a p-InP epitaxial active region, the open circuit voltage (V_{oc}) and the power conversion efficiency (η_p) of the solar cell are increased from $V_{oc} = 0.62 \pm 0.3$ V for a conventional cell to $V_{oc} = 0.75 \pm 0.3$ V for devices with a $\delta = 4$ nm thick PTCDA layer at one sun, AM1.5G simulated solar illumination. This leads to an increase in η_p from $13.2 \pm 0.5\%$ for devices without PTCDA to $15.4 \pm 0.4\%$ for devices with $\delta = 4$ nm PTCDA.

The solar cell active region was grown by gas source molecular beam epitaxy on a p-type, Zn-doped (100) InP substrate. The epitaxial structure consists of a 0.1 μm thick Be doped (3×10^{18} cm^{-3}) p-type InP buffer layer and a 4μm thick lightly Be doped (3×10^{16} cm^{-3}) absorption region. Following growth, the epitaxial wafer was cleaned by sequential immersion for 5 min in acetone, isopropanol maintained at 140 °C, and then for 1 min in 25% $NH_4OH:H_2O$ to remove the native oxide. The back contact consisted of 20 nm Pd/5 nm Zn/20 nm Pd/200 nm Au and was then alloyed at 400 °C for 1 min. Conventional InP Schottky barrier solar cells were fabricated by ITO sputter deposition through a shadow mask with 1 mm diameter circular openings. The deposition rate was 0.1 Å/s for the first 100 Å and then increased to 0.3 Å/s to achieve a total thickness of 1000 Å. The PTCDA source material was purified three times by sublimation prior to deposition.[11] Window layers from $\delta = 1$ nm to 30 nm thick were deposited by vacuum thermal evaporation at a rate of 1 Å/s in a high vacuum chamber with a base pressure $< 2 \times 10^{-6}$ Torr. The ITO sputter deposition rate and thickness for window layer devices were similar to those used for the ITO/InP diodes.

The energy level alignment at the OI interface was measured using ultraviolet photoemission spectroscopy (UPS) and X-ray photoemission spectroscopy (XPS). Photoluminescence (PL) data were obtained using a spectrofluorometer at incident and detection angles of 45°. The diode external quantum efficiency (EQE) was obtained using a monochromator, a lock-in amplifier, and a tungsten-halogen illumination source whose intensity was referenced to a calibrated Si photodetector. The current density (J) versus voltage (V) characteristics were measured using a semiconductor parameter analyzer in the dark and under simulated AM1.5G illumination. The illumination intensity was calibrated using a National Renewable Energy Laboratory Si reference solar cell.

Figure 1 shows the PL and excitation spectra of the InP epitaxial layers with and without PTCDA windows. We observe that the InP PL intensities of the PTCDA-coated samples are more than double that of bare InP. Now, the PL quantum efficiency η_{PL} is expressed as: $\eta_{PL} \propto k_{rad}/(k_{rad} + k_{nr} + k_s)$, where k_{rad} is the radiative recombination rate, k_{nr} is the nonradiative recombination rate in the bulk of the semiconductor, and k_s is the nonradiative surface recombination rate. Since short wavelength ($\lambda = 409$ nm) optical exci-

[a)]Electronic mail: stevefor@umich.edu.

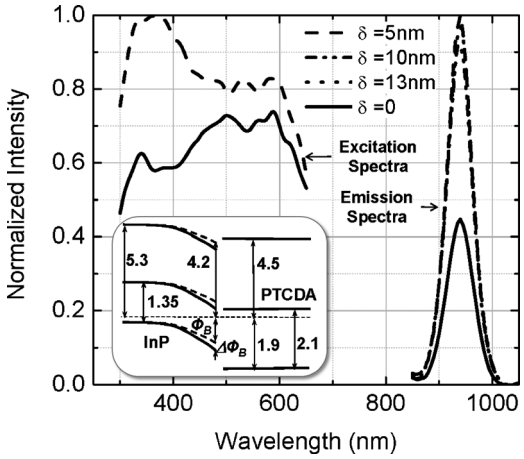

FIG. 1. Photoluminescence (excitation at λ=409 nm) and excitation (emission at λ=930 nm) spectra of a p-InP epitaxial wafer and of the same wafer with various thicknesses (δ) of 3,4,9,10-perylene-tetracarboxylic-dianhydride (PTCDA) capping layer. Inset: Energy levels of p-InP and PTCDA inferred from ultraviolet photoemission spectroscopy. Units of eV are applied to the numbers in the inset.

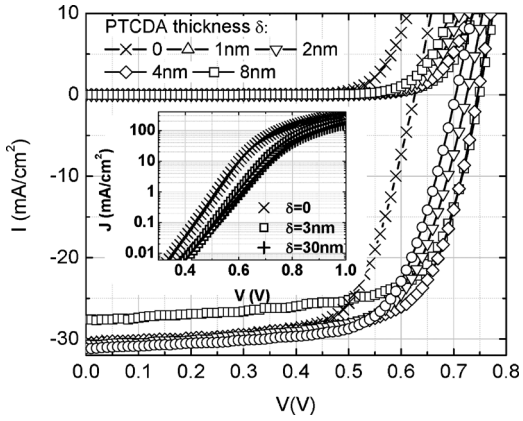

FIG. 2. Current density-voltage (J-V) characteristics of p-InP/PTCDA solar cells with PTCDA window layer thicknesses of δ=0, 1, 2, 4, and 8 nm. Inset: Measured (symbols) and fit (lines) dark J-V characteristics of p-InP/PTCDA solar cells with δ=0, 3, and 30 nm.

tation as used in Fig. 1 primarily impacts the filling of surface and near-surface defects, the enhanced PL indicates a reduced k_s. Specifically, the spectrally dependent absorption of InP suggests that the absorption length in InP at λ =900 nm is ~1 μm, while at λ=400 nm it is only ~20 nm.

When PTCDA is deposited on an InP surface, holes are injected from the PTCDA, thereby neutralizing negatively charged traps at the InP surface. This increases ϕ_B, as shown in Fig. 1, inset. As a result, the active surface trap density that accounts for the nonradiative surface recombination is reduced.

The conclusion that PTCDA reduces surface recombination is confirmed by the excitation spectra, which show that the PL intensity enhancement is significantly larger at short (λ<420 nm) than at long wavelengths (λ>580 nm), particularly when we note that δ=5 nm PTCDA may attenuate the excitation signal in the short wavelength region. It is also observed that the PL intensity of the PTCDA-capped samples increases slightly with illumination over time, indicating that surface trap filling of the deepest levels takes several minutes to complete.

The energy level diagram of the PTCDA/InP interface, inferred from UPS data, is shown in the inset of Fig. 1. As-grown p-InP exhibits a surface vacuum level at 4.2 ± 0.1 eV relative to E_F, whereas the PTCDA deposited on InP has a vacuum level at 4.5 ± 0.1 eV. The energy band bending at the InP surface is shown both before (dashed line, $\phi_B = 1.1 \pm 0.1$ eV), and after PTCDA deposition (solid line, $\phi_B' = \phi_B + \Delta\phi_B$). Here, $\Delta\phi_B$ is the incremental increase in barrier height that results from the change in the surface state charge on deposition of the PTCDA. After depositing 5 Å PTCDA, The In 3d peak in the InP XPS spectrum was shifted by 20 meV toward a higher binding energy with respect to the Fermi level, which indicates more surface band bending,[12] and $\Delta\phi_B$ is on the order of 20 meV. Since the highest occupied molecular orbital (HOMO) energy level of PTCDA is 1.9 ± 0.1 eV below E_F, the discontinuity between the valence band maximum of InP and the PTCDA HOMO is $(0.8\text{-}\Delta\phi_B)$ eV. The energy difference between the lowest unoccupied molecular orbital (LUMO) energy level of PTCDA and the InP conduction band minimum is negligible. As a result, the photogenerated electrons in window layer cells are transported from the InP to the ITO electrode through the PTCDA without encountering an energy barrier.

Figure 2 shows the J-V characteristics of InP solar cells with various δ in the dark, and under one sun, AM1.5G illumination. All devices with $\delta \leq 4$ nm show similar photocurrent densities. However, $V_{oc} = 0.62 \pm 0.3$ V for devices without PTCDA (δ=0), while $V_{oc} = 0.75 \pm 0.3$ V for those with δ=4 nm. The power conversion efficiency is correspondingly increased from $13.2 \pm 0.5\%$ for δ=0 to $15.4 \pm 0.4\%$ for those with δ=4 nm.

The forward J-V characteristics are fit using: $J = J_s[\exp\{(qV - JR_s)/nkT\} - 1]$. The fits, shown in Fig. 2 inset, yield the diode ideality factor, n, the specific series resistance, R_s, and the saturation dark current, J_s, as listed in Table I together with the measured V_{oc}. Previously, it has been shown that the OI interface can be modeled as a semiconductor heterojunction[8] to yield $J_s = J_{s,0} \exp(-\Delta\Phi_B/kT)$, where $J_{s,0}$ is the saturation dark current of the device without a PTCDA window layer. Assuming a short circuit photocurrent density of J_{sc}, we can write the V_{oc} as

$$V_{OC} = \frac{nkT}{q}\ln\left[\frac{J_{SC}}{J_s}\right] = \frac{nkT}{q}\ln\left[\frac{J_{SC}}{J_{s,0}}\right] + n\Delta\Phi_B$$

In InP-PTCDA devices, the increase in V_{oc} is due to both a reduced J_s and an increased n. The reduction in J_s results from the increased Schottky barrier height with PTCDA deposition. The increased n is attributed to a reduced forward bias voltage across InP due to the drop across PTCDA. Note

TABLE I. Dark current fitting parameters.

δ (nm)	n	R_s ($\Omega \cdot cm^2$)	J_s ($\times 10^{-10}$ A/cm^2)	V_{oc} (V)
0	1.31	0.80	4.8	0.62
1	1.43	1.3	1.5	0.71
3	1.47	0.86	1.5	0.75
5	1.56	0.75	4.0	0.75
10	1.56	0.83	2.6	0.76
30	1.59	1.0	3.6	0.76

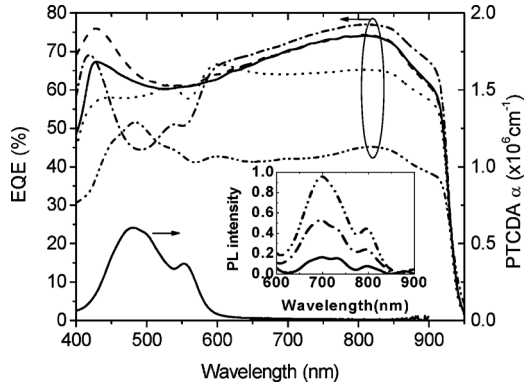

FIG. 3. External quantum efficiency (EQE) vs wavelength for p-InP/PTCDA solar cells with PTCDA layer thicknesses of δ=0 (solid line), 3, (dash), and 10 nm (dot). The PTCDA absorption spectrum is shown as a reference. The EQE of devices with 24 nm thick bathocuproine (BCP) (dash dot) and 30 nm MoO_3 (dash dot dot) exciton blocking layers (EBLs) between PTCDA and ITO are also shown. Inset: Photoluminescence of PTCDA in the Quartz/PTCDA/exciton blocking layer (EBL)/ITO structures with no EBL (solid line), with 12 nm BCP (dash dot), and with 30 nm MoO_3 (dash dot dot).

that R_s does not increase with the increased δ, resulting in the same fill factor for devices with and without PTCDA.

Figure 3 shows the EQE versus λ for various δ. For $\delta < 3$ nm, the EQE is close to that of the ITO/InP solar cell at $\lambda > 500$ nm. However, at shorter wavelengths, the EQE for PTCDA capped cells is increased due to increased PTCDA transparency and reduced surface recombination. When δ=10 nm, the EQE is significantly decreased in the PTCDA absorption region between λ=420 and 580 nm. Measurements of PTCDA PL on quartz substrates indicate that excitons generated in PTCDA are quenched by ITO deposited on its surface, as inferred from the PL spectra for these samples in Fig. 3, inset. To reduce quenching, a bathocuproine (BCP) or MoO_3 exciton blocking layer (EBL) is sandwiched between the PTCDA and the ITO cathode, resulting in a significant increase in PTCDA PL intensity. When BCP is employed in a window layer solar cell, the EQE loss at λ=480 nm disappears, whereas the use of MoO_3 results in a *peak* at this wavelength that corresponds to the PTCDA absorption maximum. These results indicate that excitons in an organic (e.g., PTCDA) can dissociate at its interface with an inorganic semiconductor (InP), ultimately contributing to an increased solar cell efficiency beyond that obtained with a conventional, "passive" window layer.

The stability of the PTCDA-InP devices has not been systematically tested, although we see no degradation in performance after exposure to air for several days. This is consistent with the observation that PTCDA is a highly stable organic compound.

In summary, we have found that PTCDA can be used as a window layer that both decreases the recombination rate while generating photocurrent due to exciton dissociation at the InP surface in an ITO/PTCDA/InP solar cell. The solar cell power conversion efficiency is increased from $13.2 \pm 0.5\%$ to $15.4 \pm 0.4\%$ by using a 4 nm thick PTCDA window layer, largely due to a concomitant increase in V_{oc} that arises from neutralizing InP surface states.

The authors thank the U.S. Department of Energy, Energy Frontier Center at the University of Southern California (Grant No. DE-SC0001011, CKR), the Air Force Office of Scientific Research (NL), and Global Photonic Energy Corp. (SRF, XX) for their generous support of this work.

[1]D. L. Pulfrey, IEEE Trans. Electron Devices **25**, 1308 (1978).
[2]H. J. Hovel and J. M. Woodall, J. Electrochem. Soc. **120**, 1246 (1973).
[3]R. K. Jain and G. A. Landis, Appl. Phys. Lett. **59**, 2555 (1991).
[4]M. A. Green, F. King, and J. Shewchun, Solid-State Electron. **17**, 551 (1974).
[5]M. A. Green, A. W. Blakers, and C. R. Osterwald, J. Appl. Phys. **58**, 4402 (1985).
[6]E. Yablonovitch, T. Gmitters, R. M. Swanson, and Y. H. Kwark, Appl. Phys. Lett. **47**, 1211 (1985).
[7]M. Taguchi, K. Kawamoto, S. Tsuge, T. Baba, H. Sakata, M. Morizane, K. Uchihashi, N. Nakamura, S. Kiyama, and O. Oota, Prog. Photovoltaics **8**, 503 (2000).
[8]S. R. Forrest, M. L. Kaplan, and P. H. Schimt, J. Appl. Phys. **55**, 1492 (1984).
[9]S. R. Forrest, M. L. Kaplan, and P. H. Schimt, J. Appl. Phys. **56**, 543 (1984).
[10]V. Gowrishankar, S. R. Scully, M. D. McGehee, Q. Wang, and H. M. Branz, Appl. Phys. Lett. **89**, 252102 (2006).
[11]S. R. Forrest, Chem. Rev. **97**, 1793 (1997).
[12]T. Chassé, C.-I. Wu, I. G. Hill, and A. Kahn, J. Appl. Phys. **85**, 6589 (1999).